Available online at www.sciencedirect.com

ScienceDirect

Energy Procedia 49 (2014) 1061 – 1070

Energy Procedia

SolarPACES 2013

PCM storage system with integrated active heat pipe

R. Yogev[a], A. Kribus[a]*

[a] School of Mechanical Engineering, Tel-Aviv University, Tel-Aviv 69978, Israel

Abstract

The use of the latent heat of phase change materials (PCM) is considered a promising approach to store heat at a nearly constant temperature for direct steam generation (DSG), but the poor thermal conductivity of commonly available storage materials imposes severe limitations on storage performance. A new method is proposed to overcome the limitations of the low thermal conductivity. The approach is to physically decouple the evaporator pipes from the PCM, thus allowing independent sizing of each component. The thermal link between the two components is done via evaporation and condensation of a heat transfer fluid (HTF), according to the principle of a heat pipe. Pumping the liquid HTF provides active control of the heat pipe operation. The new concept is modeled and compared to the conventional design of conduction based PCM annulus around the steam pipe. An example case shows a significant advantage in performance of the active heat pipe configuration due to its reduced thermal resistance.

Selection and peer review by the scientific conference committee of SolarPACES 2013 under responsibility of PSE AG.
Final manuscript published as received without editorial corrections.
Keywords: Phase change materials (PCM); Latent heat thermal storage (LHTS); Heat pipe; Concentrating solar power (CSP)

1. Introduction

One of the major challenges of solar energy production is the intermittency in the availability of solar radiation. The need for a reliable energy source past sunset and during sporadic cloudy periods makes it difficult to rely on solar power plants as a major source. This problem could be greatly mitigated by introducing a heat storage system into large scale solar thermal plants. Numerous solutions have been proposed and investigated [1] including various types of chemical and thermal storage systems. Latent heat thermal storage (LHTS) is one promising approach,

* Corresponding author. Tel.: +972-3-6405924;
E-mail address: kribus@tauex.tau.ac.il

Selection and peer review by the scientific conference committee of SolarPACES 2013 under responsibility of PSE AG.
Final manuscript published as received without editorial corrections.
doi:10.1016/j.egypro.2014.03.115

where heat from the solar field is used to melt a store of phase change material (PCM) during charging. In discharge, the PCM is solidified, thus delivering its heat of phase transition to the thermal process. This type of storage provides high thermal capacity per unit mass, and is advantageous for steam production (e.g., in a Rankine cycle power plant) due to the isothermal nature of the process. In a power plant that requires superheat, a separate unit is added with sensible heat storage (using, for example, concrete or molten salt) to provide heat for superheating of the steam [2]. In this work it is assumed that such a sensible heat unit exists but it is not analyzed here. A major inhibition for the PCM storage unit is the typically low thermal conductivity of storage materials available at high temperatures. The low thermal conductivity leads to a steep decrease with time of the power extracted from storage, and compensating for this effect requires plant operation at sliding pressure mode and reduced thermodynamic efficiency [3]. Several methods were proposed to overcome this problem, including additives in the PCM to enhance its thermal conductivity, and various fin geometries [4,5].

Nomenclature

A	Area (m^2)	*Subscripts*	
d	Steam pipe diameter (m)		
C	Heat capacity (J kg^{-1} K^{-1})	*0*	Process start
g	Earth's gravity constant (m s^{-2})	*l*	Liquid HTF
h	Latent heat (J kg^{-1})	*lv*	HTF phase transition
k	Thermal conductivity (W m^{-1} K^{-1})	*m*	Melting
m	Mass (kg)	*p*	PCM
$\dot{m}$	Mass flow rate (kg s^{-1})	*s*	Steam property
q	Heat flux (W m^{-2})	*sat*	Steam saturation
R	Thermal resistance (m^2 KW^{-1})	*sp*	Steam pipe
T	Temperature (K)	*struc*	Structural materials
t	Time (s)	*v*	Vapor HTF
x	Steam quality (–)	*w*	PCM slab wall
y	Vertical coordinate along PCM slab (m)	*wo*	Outer pipe wall
z	Horizontal coordinate along steam pipe (m)	*wi*	Inner pipe wall

Greek

β	Thermal power reduction rate (–)
δ	HTF film thickness (m)
μ	Dynamic viscosity (kg m^{-1} s^{-1})
ξ	Solid/liquid boundary position (m)
ρ	Density (kg m^{-3})
τ	Typical discharge time (s)

In this work, a different approach is presented to improving the thermal performance of the storage. We propose to reduce the impact of the low thermal conductivity of the PCM by physically decoupling the areas for heat transfer on the steam side and the PCM side. This allows independent sizing, producing a larger heat transfer area and a shorter path for conduction on the PCM side. The transport between the two decoupled elements is done with evaporation and condensation of a heat transfer fluid (HTF), which is equivalent to a heat pipe mechanism. An additional element of the proposed solution is active operation by pumping of the liquid HTF, leading to a controllable and reversible operation for charge and discharge modes. A similar solution with evaporation and condensation was proposed [6] but it was based on passive reflux without active pumping. A passive reflux heat pipe was also proposed for solar receivers in space power applications [7] and terrestrial dish-Stirling systems [8].

Here we analyze the operation of the proposed storage only in discharge, which is the more problematic mode in terms of maintaining the desired output power. A model is presented of the storage module with active heat pipe and

the thermodynamic cycle. A representative example of storage and cycle performance is presented, showing a potential to improve the thermodynamic performance of the entire plant compared to previous storage solutions.

2. Concept and method

2.1. Storage configuration

The active heat pipe storage system comprises water/steam pipes and PCM capsules as separate elements not in physical contact with each other. This allows assigning a much larger heat transfer area to the PCM side, while maintaining a relatively small amount of high pressure steam pipes. Fig. 1 shows schematically the major components of the system.

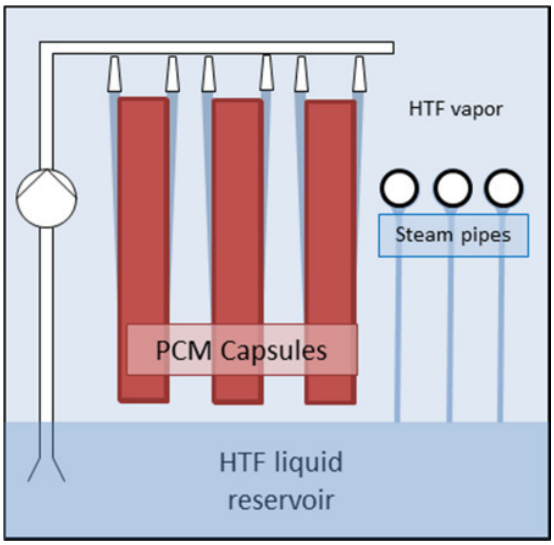

Fig. 1 – Storage system scheme in discharge mode

The PCM capsules have a generally flat shape, with high surface area and low thickness, providing a short path for conduction heat transfer through the PCM. Both the PCM capsules and the steam pipes are inside a sealed container filled with a heat transfer fluid (HTF) in a state of saturation, with liquid and vapor in equilibrium. A circulation system is provided in the container with a pump, pipes, and a control system in order to circulate the liquid HTF to the surfaces of either the PCM capsules or the steam pipes. During charging, the HTF pressure is adjusted such that its saturation temperature is slightly higher than the PCM melting temperature, but lower than the saturation temperature of the steam arriving from the solar collector field. The pump is operated to provide saturated liquid HTF over the steam pipes. The HTF evaporates on the steam pipes and condenses over the PCM capsules. During discharge, the HTF pressure is adjusted such that its saturation temperature is slightly lower than the PCM melting temperature, but higher than the saturation temperature of the water to be evaporated. The pump is operated to provide saturated liquid HTF over the PCM capsules. The HTF evaporates on the PCM capsules and condenses over the pipes. In both modes the vapor HTF flows from side to side as needed by free convection, over a large cross section area that does not restrict its flow, in contrast to traditional heat pipes that have a restrictive small cross section area.

The active heat pipe storage requires a suitable HTF that provides the needed saturation temperature at reasonable pressure near atmospheric pressure, to avoid the need of a high-pressure container. For the standard solar Rankine cycle with PCM melting temperature around 300°C, we examined the performance of the proposed storage module using Therminol VP-1 as HTF. This material is perhaps not ideal for a real system, since it is flammable,

toxic and is chemically unstable in high temperatures. However, it is used here as an example for the analysis of the thermodynamic behavior, while for future practical applications, other materials should be sought.

2.2. Model setup

The model is based on several simplifying assumptions, the main ones being: constant PCM melting temperature; all HTF is at saturation temperature; no presence of incondensable materials in the HTF container; negligible pressure drop in the HTF flow; one-dimensional heat transfer in the PCM capsule and in the pipe; quasi-steady-state; and negligible heat loss to the environment. The physical decoupling of the PCM from the steam pipes allows separate formulation of the heat transfer processes on the steam side and on the PCM side. These two separate sets of formulae are later coupled to solve the complete problem. The model described here refers only to the discharge process of the storage.

2.3. PCM capsule heat transfer

During storage discharge, liquid HTF at saturation conditions is provided at the top of the PCM slab creating a falling film. This liquid film is cooler than the PCM, causing the PCM to solidify while the liquid evaporates. The heat then flows through three thermal resistances in series: the falling film, the capsule wall, and the solidified PCM layer. The thermal resistance of the capsule wall is represented in the initial condition. A momentum balance on the falling film produces a differential equation for the falling film thickness $\delta(y)$ [9]:

$$\frac{\partial \delta^3}{\partial \mathrm{y}} = \frac{1}{\delta}\left[\frac{3\mu_l}{g\rho_l(\rho_l-\rho_v)}\right]\frac{k_l}{h_{lv}}\left[T_v - T_w(y,t)\right] \tag{1}$$

An energy balance on the PCM leads to the equation for the advancement of the PCM moving solidification front [3]:

$$\rho_p h_m \frac{\partial \xi}{\partial \mathrm{t}} = \frac{k_p\left[T_m - T_w(y,t)\right]}{\xi(y,t)} \tag{2}$$

The heat extracted from the PCM equals the heat transferred to the film, leading to a coupling of equations (1) and (2) via the PCM module's external wall temperature T_w:

$$T_w(y,t) = \frac{\delta(y,t)k_p \cdot T_m + \xi(y,t)k_l \cdot T_v}{\delta(y,t)k_p + \xi(y,t)k_l} \tag{3}$$

This completes the set of equations that describe the position of the moving solidification front in the PCM as a function of time $\xi(t)$ and the thickness of the HTF film as a function of vertical position and time $\delta(y,t)$. In practice, when substituting typical parameter values, the change in film thickness is very small and has a negligible effect on the rate of heat transfer. This has been validated for several sets of data [10]. Therefore, the model can be simplified using the approximation of uniform thermal resistance of the film. This reduces equations (1) and (2) to:

$$q_p(t) = \rho_p h_m \frac{\partial \xi}{\partial \mathrm{t}} = \frac{\left[T_m - T_w(y,t)\right]}{\xi(t)/k_p + R(t)} \tag{4}$$

R(t) is the thermal resistance of the liquid film, which depends on time due to the variations in HTF temperature during discharge that affect its thermal conductivity. With this approximation, the amount of HTF evaporated from one face of a single slab is:

$$\dot{m}_{lv} = \frac{A \cdot q_p(t)}{h_{lv}} \tag{5}$$

2.4. Water-Steam pipe heat transfer

Heat transfer in the steam pipes consists of three thermal resistances in series: free convection condensation of the HTF on the external part of the pipe, conduction through the pipe wall, and forced convection boiling within the pipe. We use Nusselt's correlation for the heat transfer coefficient in condensation on horizontal pipes [11]:

$$q_s(z) = 0.725\left\{\frac{g\rho_l(\rho_l - \rho_v)\cdot h_{lv}k_l^{\,3}[T_v - T_{wo}(z)]^3}{d_{wo}\mu_l}\right\} \tag{6}$$

Though dropwise condensation is characterized with higher heat transfer coefficients and is therefore preferable over film condensation, it is difficult to model and strongly affected by temperature, pipe material and surface finish. The performance considering filmwise condensation is therefore a conservative model, which is likely to be surpassed in an actual system.

The temperature difference across the pipe wall is, from Fourier's law:

$$T_{wo}(z) - T_{wi}(z) = \frac{\overline{q}_{wi} d_{wi} \cdot \ln\left(\frac{d_{wo}}{d_{wi}}\right)}{2k_{sp}} \tag{7}$$

Forced convection boiling heat transfer within the pipe is evaluated using a method suggested in [12] and will not be discussed here. One notable detail is that the heat transfer coefficient is dependent on steam quality, meaning that heat flux varies along the pipe, affecting both the inner and outer wall temperatures. From [12], the local heat flux could be represented as a function of the inner wall temperature, water saturation temperature and steam quality:

$$q_s = q_{wi} = q_s(T_{wi}(t), T_{sat}(t), x(z)) \tag{8}$$

This, in combination with equations (6),(7) allows solving for local wall temperatures and heat flux given water and HTF saturation temperatures.

2.5. Overall balance and power block model

Since the HTF is considered to be at saturation temperature, the entire thermal power discharged from the PCM contributes solely to HTF evaporation. Similarly, subcooling of HTF that condenses over the steam pipes is neglected. This approximation can be evaluated by estimating the ratio between the sensible and latent heat extracted from the HTF using the Jakob number:

$$Ja = \frac{C(T_v - T_{wo})}{h_m} \tag{9}$$

The temperature difference that was used in this estimate is between the HTF vapour and the external face of the steam pipes. In all the case studies examined in this work $Ja \le 0.021$, and therefore neglecting of sensible heat is acceptable. The total thermal power discharged from the PCM capsules then equals the total power transferred to the water in the pipes. The ratio of the surface area of the PCM capsules to the area of the steam pipes A_p/A_{sp} is defined as a major design input, and this ratio determines the heat fluxes and temperature differences on the two sides of the process. Given material properties and the geometry of the system, four parameters are left as variables: the HTF

and steam saturation temperatures, and the heat flux values at the PCM capsule wall and into the steam $T_{lv}(t)$, $T_{sat}(t)$, $q_p(t,y)$ and $q_s(t,z)$ respectively. Setting the value for one of these parameters defines the other three via the relations described in equations (1)-(8). With $T_{sat}(t)$ and $q_s(t,z)$ known, it is possible to address the performance of the thermodynamic cycle.

Steam generated by the PCM storage is superheated by a separate sensible heat storage unit, which is not addressed in this work, and then fed into the turbine inlet. The performance of the turbine is affected by the steam pressure that corresponds to T_{sat} and by the steam mass flow rate, defined by $\overline{q}_s$. The detailed thermodynamic analysis of the power cycle has been presented in a previous work [3] and assumes a fixed turbine isentropic efficiency.

2.6. Numerical solution

The set of equations presented above was solved numerically using "Matlab" computer software. The inputs of the numerical model include material properties of the PCM, HTF and water, as well as the geometry of the system and the desired heat flux from the PCM wall. The model was solved as a quasi-steady-state problem over short time increments. For every time increment, heat flux on the face of the PCM slabs and the corresponding HTF evaporation rate were calculated from equations (4,(5). By multiplying the heat flux with the PCM surface area, we get the instantaneous discharge power. Applying the assumption of negligible thermal losses, this equals the thermal power that is transferred to the steam. Solving equations (6-(8) determines the steam evaporation temperature, the steam pressure and the steam evaporation rate.

3. Results and discussion

3.1. Case study description

It is most desirable to examine system feasibility without requiring the development of new materials. For this reason, the model has been solved using the properties of the common PCM sodium nitrate ($NaNO_3$) as storage material [13] and of the two-phase thermal fluid Therminol VP-1 [14] as HTF, both satisfying the requirements presented in Section 2.1. Key parameters, including material properties and element sizing are reported inTable 1.

Table 1 – Case study parameters

Property	Symbol	Value
PCM Density	ρ	1900 kg m^{-3}
PCM Heat of Fusion	h_m	176 kJ kg^{-1}
PCM Melting Temperature	T_m	306℃
PCM Thermal Conductivity	k_p	0.514 (mK)$^{-1}$
Nominal Discharge Time	τ	2 hours
Nominal Discharge Flux	q_0	1000 W m^{-2}
PCM Slab Thickness	-	4.3 cm
Total PCM slabs area	A_p	400 m^2
HTF film thickness	-	0.5 mm
Number of steam pipes	-	40
Steam pipe length	L	25 m
Steam pipe internal diameter	-	1.58 cm
Steam pipe external diameter	-	2.13 cm

Steam and HTF properties vary with temperature and pressure and are determined from [15] and [16] respectively. The dimensions of the steam pipe are those of a schedule 40 seamless stainless steel pipe with a nominal diameter of 1/2" [17].

As the PCM storage is discharged, a gradually increasing layer of solid PCM is formed on the boundary of the slab. This translates to an increase in the thermal resistance of the system that leads to a reduction in thermal power, an increase in the temperature difference, or a combination of the two. Previous work [3] discussed different operation strategies of the thermodynamic cycle, and their impact on the variation in time of the thermal power extracted from storage and the electrical power produced. Here we apply two operation scenarios: first with thermal power linearly changing with time (including the case of zero change rate, i.e., constant thermal power); and second with thermal power varying so as to produce a constant electrical power.

3.2. Linearly decreasing thermal power

In this scenario, the saturation temperatures of the HTF and water are controlled to sustain a linear reduction in thermal power. The rate of reduction is defined by the dimensionless parameter β, which represents the fraction of power reduction at the end of the nominal discharge time τ:

$$\frac{Q_{th}(t)}{Q_{th,0}} = 1 - \beta \frac{t}{\tau} \tag{10}$$

The special case of $\beta = 0$ represents discharge at a constant thermal power. Fig. 2 shows the relative reduction with dimensionless time in electrical power for three values of β. Achieving smaller values of β requires a larger reduction rate in HTF and water saturation temperatures to compensate for the increasing thermal resistance of the PCM. This leads to a higher decrease in the thermodynamic cycle efficiency. Therefore, discharge at a constant thermal power cannot provide constant electrical power, as also shown in [14] for conventional storage configurations.

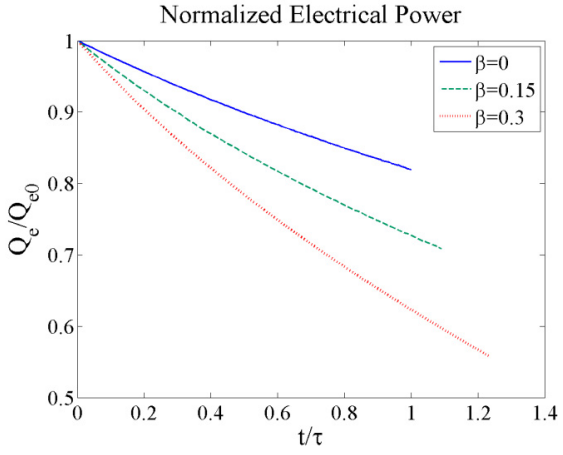

Fig. 2 – Operation at linearly decreasing heat flux

The total amount of electrical energy produced throughout discharge depends on the operation strategy. This could be quantified as the "discharge efficiency" (DE): the total electricity produced as a fraction of the electricity that would have been produced if the solid PCM had infinite thermal conductivity. In the ideal case, the electrical power production would remain constant at nominal value for the entire nominal storage time.

$$DE = \frac{\int_0^{t_{tot}} Q_e(t)dt}{\tau \cdot Q_{e,0}} \tag{11}$$

The corresponding DE values for the three cases from Fig. 2 are given in Table 2. In all cases the electricity produced from storage is less than the potential of an ideal PCM. Higher values of β produce higher DE, but at the cost of higher variability over a longer discharge time. In constant thermal power operation about 10% of the potential to produce electricity is lost due to the reduction in cycle efficiency while operating at lower steam pressure.

Table 2 – Discharge efficiency (DE) values

Case	DE
β=0	0.903
β=0.15	0.929
β=0.30	0.931

3.3. Constant electrical power

As demonstrated in the previous section, maintaining a constant thermal discharge power does not provide constant electrical power due to the reduced thermodynamic efficiency of the cycle. This effect can be compensated by a further increase in the temperature difference, which causes the thermal power to increase in time. Fig. 3 presents the required increase in thermal power and in steam mass flow rate, and the corresponding decrease in the cycle's thermodynamic efficiency, when operating at constant electrical power. The first two are normalized by their nominal values and the latter is presented at its absolute value and plotted against the secondary vertical axis.

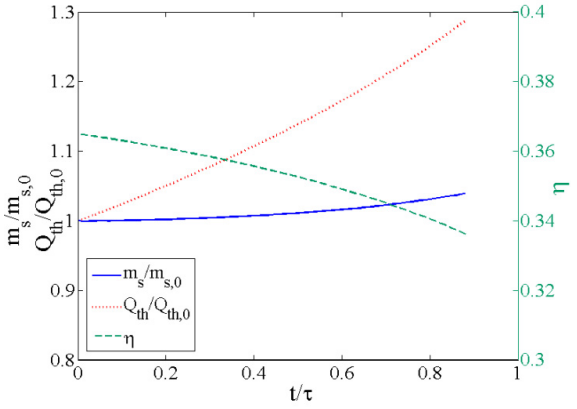

Fig. 3 – Steam mass flow rate, thermal power and thermodynamic efficiency at constant electrical power operation

The required increase in thermal power is significant, due to the increasing thermal resistance faced by the solid PCM as well as the higher heat of evaporation at the reduced water pressure. The constant electrical power generation is achieved with a penalty of increased loss, with discharge efficiency of $DE = 0.889$, which can also be observed as shorter discharge time of about 11% less than the nominal value. It is interesting to note that in spite of the significant increase in thermal power and the significantly shorter discharge period of this case compared to the case of constant thermal power, the DE is almost the same (the difference is only 1.4%). Therefore, operation at constant electrical power does not require a significant further penalty compared to operation at constant thermal power.

3.4. Comparison to standard storage geometry

We compare the performance of the active heat pipe storage system to the simpler reference configuration composed of steam tubes surrounded by PCM annuli, with one-dimensional conduction heat transfer in the radial direction [3]. For both systems, the same steam pipes were used, and the same amount of PCM per unit steam pipe length. Hence, the reference geometry of the PCM is an annulus with internal diameter 2.13 cm and an external

diameter of 7.4 cm. The discharge of the reference system is determined using a heat balance between the solidifying PCM and evaporating steam; details are given in [3]. Fig. 4 compares the normalized electrical power output of the two storage configurations, both operated in constant thermal power mode (β=0). The heat pipe system offers a major improvement with respect to the radial conduction configuration, where the electrical power output drops by only 18% at the end of discharge, compared to 35% for the radial system.

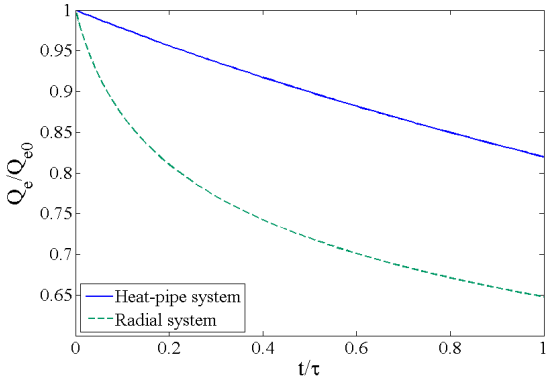

Fig. 4 – Normalized electrical power output for the two storage configurations, both operated in constant thermal power mode

Another aspect for comparison is the required heat transfer area per unit volume of storage material. In the case study presented here, this ratio is 46.5 m^2/m^3. For comparison, in the conduction-based finned tube storage system presented in [18], a much higher surface area was used, about 200 m^2/m^3.

4. Discussion

The active heat pipe configuration of PCM thermal storage has a potential to mitigate the effect of low thermal conductivity of the PCM. The physical decoupling of the PCM heat transfer area from the geometry of the steam pipes allows an additional degree of freedom for shaping PCM capsules and reducing the impact of thermal conduction. The thermal simulation shows that a storage system with the active heat pipe can achieve significantly higher performance compared to the more traditional conduction-based configurations. In constant thermal power discharge, the active heat pipe system maintains lower temperature differences, higher steam pressure, and higher thermodynamic efficiency and electrical power output. These advantages imply higher storage efficiency regardless of the discharge regime. For example, if constant electrical power is desired, the active heat-pipe system should allow a longer discharge period at the nominal power compared to an equivalent conduction-based storage system discharged in a similar manner. The analysis of the constant electrical power mode is currently underway.

The mass of the PCM in the case study above is 2.7 times the mass of the pipes, a ratio that may be increased in future optimization for cost reduction. A higher PCM mass fraction in the radial conduction configuration will reduce the cost of the steel pipes per unit stored energy, but will also reduce the system performance due to increased thermal resistance in the thicker PCM layer. In the active heat pipe system, on the other hand, it is possible to increase the PCM mass fraction by adding PCM capsules without a significant change in the heat transfer performance. Note that the heat pipe system analysis used only natural PCM properties; combining conductivity enhancements in the PCM capsules with the heat-pipe storage may further reduce the amount of structural materials required while maintaining satisfactory performance.

The active heat pipe requires additional elements in the storage system, including: a pump, HTF distribution piping, and a control system. However, these elements are implemented standard technology that is ubiquitous in any power plant and do not represent a significant addition of cost or risk. Therefore the added complexity of an active vs. passive storage system may be a reasonable investment to achieve the significant potential gain in power generation.

The model presented here is simplified and is intended only as a preliminary evaluation of the thermodynamic feasibility of the active heat pipe approach. A more detailed engineering and cost model should be used for a more detailed evaluation, and obviously an experimental validation is needed for the operation of the proposed heat pipe geometry.

Acknowledgment

This work was supported by a grant from the Ministry of Science and Technology, Israel, and by the Ministry of Foreign Affairs and the Ministry of National Education and Research, France.

References

[1] A. Gil, M. Medrano, I. Martorell, A. Lázaro, P. Dolado, B. Zalba, et al., State of the art on high temperature thermal energy storage for power generation. Part 1—Concepts, materials and modellization, Renewable and Sustainable Energy Reviews. 14 (2010) 31–55.
[2] D. Laing, C. Bahl, T. Bauer, D. Lehmann, W.-D. Steinmann, Thermal energy storage for direct steam generation, Solar Energy. 85 (2011) 627–633.
[3] R. Yogev, A. Kribus, Operation strategies and performance of solar thermal power plants operating from PCM storage, Solar Energy. 95 (2013) 170–180.
[4] L. Fan, J.M. Khodadadi, Thermal conductivity enhancement of phase change materials for thermal energy storage: A review, Renewable and Sustainable Energy Reviews. 15 (2011) 24–46.
[5] M. Liu, W. Saman, F. Bruno, Review on storage materials and thermal performance enhancement techniques for high temperature phase change thermal storage systems, Renewable and Sustainable Energy Reviews. 16 (2012) 2118–2132.
[6] R. Adinberg, D. Zvegilsky, M. Epstein, Heat transfer efficient thermal energy storage for steam generation, Energy Conversion and Management. 51 (2010) 9–15.
[7] J.B. Kesseli, D.E. Lacy, The Cavity Heat Pipe Stirling Reciever for Space Solar Dynamics, in: IECEC-89, Washinton, DC, 1989: pp. 931–936.
[8] D. Laing, M. Pålsson, Hybrid Dish/Stirling Systems: Combustor and Heat Pipe Receiver Development, Journal of Solar Energy Engineering. 124 (2002) 176.
[9] A. Faghri, Y. Zhang, Transport phenomena in multiphase systems, Academic press, Amsterdam, 2006.
[10] R. Yogev, Latent Heat Storage in Solar Thermal Power Plants, Tel Aviv University, 2013.
[11] J.P. Holman, Heat Transfer, 10th ed., McGrew-Hill, 2009.
[12] R.W. Bjorge, G.R. Hall, W.M. Rohsenow, CORRELATION OF FORCED CONVECTION BOILING HEAT TRANSFER DATA, International Journal of Heat and Mass Transfer. 25 (1982) 753–757.
[13] R. Tamme, T. Bauer, J. Buschle, D. Laing, W. Steinmann, Latent heat storage above 120C for applications in the industrial process heat sector and solar power generation, 032736017 (2008) 264–271.
[14] R. Yogev, A. Kribus, Performance of Solar Thermal Power Plants Operating from PCM Storage, in: SolarPACES, Marrakech, Morocco, 2012.
[15] M. Holmgren, X Steam, thermodynamic properties of water and steam, (2007).
[16] Therminol VP-1 datasheet, downloaded from: http://www.therminol.com/pages/products/vp-1.asp, (n.d.).
[17] ASME Code for pressure piping, B31, an american national standard, 2004, (n.d.).
[18] R. Bayón, E. Rojas, L. Valenzuela, E. Zarza, J. León, Analysis of the experimental behaviour of a 100 kWth latent heat storage system for direct steam generation in solar thermal power plants, Applied Thermal Engineering. 30 (2010) 2643–2651.